Temporal evolution of surface and grain boundary area in artificial ice beads and implications for snow chemistry

Surface snow is a chemically active medium (Domine and Shepson, 2002). It exerts a major effect on overall snow chemistry and can alter the composition of the overlying air mass. This in turn can affect air quality and climate (Grannas and others, 2007). Chemically reactive trace gases and impurities are typically located on the surface of ice and in grain boundaries (GBs) (Domine and others, 2008). Field and laboratory measurements have shown that the morphology and surface area (SA) of ice crystals strongly influence trace gas exchange with the atmosphere during snow metamorphism (Domine and others, 2008). The exact role of GBs in snow and ice chemistry, however, is not well understood (Domine and others, 2008; Barret and others, 2011). Earlier work concerning the adsorption of acetone onto packed single-crystalline ice and packed ice beads did not specifically address the role of GBs in surface chemistry (Bartels-Rausch and others, 2004).

We define a GB as an interface between two ice crystals aligned in different crystal orientations. The observation that acidic trace gases accumulate along GBs in natural snow has led to the suggestion that GBs provide an extensive surface area for reactions with trace gases and impurities (Mulvaney and others, 1988; Huthwelker and others, 2006). The total

grain boundary area (GBA) is therefore an important chemical parameter of snow.

Artificial ice beads are often used as a substitute for natural snow in laboratory experiments. This correspondence reports the structural evolution of ice beads stored at two constant temperatures (–5°C and –20°C) over a 7 month period. We measured volume density and specific surface area (SSA) with X-ray tomography (μCT). The GBA was characterized using polarized light microscopy and stereology. The artificial snow consisted of ice beads measuring 0.5–0.6 mm in diameter, similar to those used in laboratory experiments concerning the partitioning of trace gases between ice and air (Bartels and others, 2002; Bartels-Rausch and others, 2004; Kerbrat and others, 2010). Accurate determinations of the SSA and density of samples are critical in comparing the structure of the artificial material to that of natural snow. Hitherto, the role of GBA in uptake of trace gases and other reactions has been largely a matter of speculation (Kerbrat and others, 2010).

In atmospheric science, the term GB refers exclusively to ice–ice interfaces. The different types of interfaces described here are shown in Figure 1. The GBA is geometrically measured as the diameter of the neck between individual ice beads (Theile and Schneebeli, 2011). The visible neck is often one of several types of GB present in a given sample. We differentiated between GBs evident as visible necks and GBs inside the ice beads that are not geometrically evident. This second type of GB is referred to as an internal GB. The total area covered by internal GBs defines an internal grain boundary area (IGBA). The ice beads used here were mainly polycrystalline. In natural snow, polycrystalline morphology is characteristic of wet or wind-transported snow. Snow composed of small rounded grains is typically monocrystalline.

The ice beads were prepared from Milli-Q-water droplets frozen in liquid nitrogen. Following freezing, ice beads were immediately sieved to collect the 0.5–0.6 mm diameter fraction. The ice beads were loaded into μCT-specific sample cylinders 20 mm in diameter and 5 cm high, and into 3 cm × 1 cm containers used for thin-section mounting and microscopic analysis. Samples were then separated into two fractions stored at temperatures of –5°C and –20°C. Both fractions were stored in isothermal boxes that maintained constant temperatures in and around the samples to adjust for small temperature variations within the storage freezer. Sample storage followed the same protocol used by Löwe and others (2011). Each month, samples from the –5°C and –20°C fractions were retrieved for μCT scanning and microscopic analysis.

Samples remained in the initial sample containers throughout the experiment in order to prevent disturbance. For μCT analysis, the sample container was placed in a secondary sample holder (20 mm diameter) and then loaded into the μCT. The three-dimensional image resolution was 10 μm over a $4.16 \times 4.16 \times 4.16 \, \text{mm}^3$ sample volume. The SSA and the volume density of the samples were determined according to methods used by Kerbrat and others (2008).

Three thin sections were evaluated per sample. Thin sections were prepared using uniform vertical section sampling and imaged under polarized light. Approximately 20 images were collected per thin section and analysed stereologically. This technique captured structures containing 180–250 ice beads per sample. The specific area per
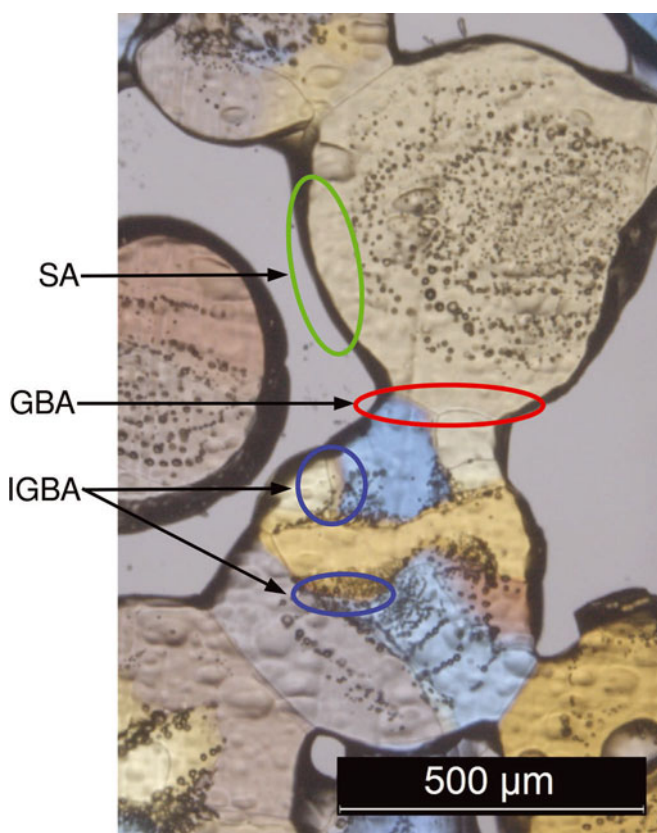
Fig. 1. Polarized light images of ice beads. The blue ellipse indicates an example of internal grain boundary area (IGBA), the red ellipse indicates grain boundary area (GBA; between two ice beads) and the green ellipse indicates surface area (SA; interface between ice and air). Both monocrystalline and polycrystalline beads are present.
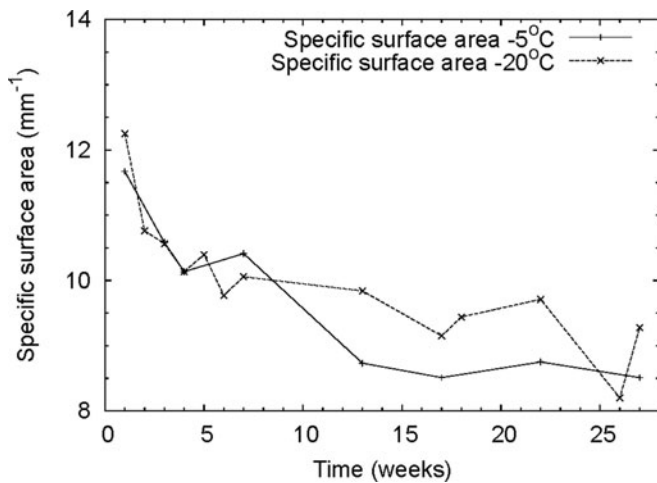
Fig. 2. Evolution of SSA for ice beads stored at –5°C and –20°C.

Fig. 3. Evolution of specific GBA for ice beads stored at –5°C and –20°C. SGBA: specific grain boundary area; SIGBA: specific internal grain boundary area.

volume of the structure of interest is given by

$$S_{ice} = \frac{2I}{(l/p)P_{ice}} \, (mm^{-1}),$$

where I is the number of intersections between the test lines and the structure of interest – SA, GBA or IGBA – l/p is the length of the test line per point, and P_{ice} is the number of touch points within the ice structure (methods detailed in Tschanz and others, 2011; Riche and Schneebeli, in press). To obtain the specific area per ice volume $(cm^2 \, g^{-1})$, specific area S_{ice} (m^{-1}) is divided by ρ_{ice}, where ρ_{ice} is the density of ice $(g \, cm^{-3})$.

TEMPORAL EVOLUTION OF ICE STRUCTURE

We found that both polycrystalline and monocrystalline morphologies were present in the ice-bead samples throughout the 27 week observation period (Fig. 1). The percentage of polycrystalline ice beads (polycrystalline ice beads/total number of ice beads) remained constant between 60% and 70% for both the –5°C and –20°C sample sets.

SSA decreased by 10–20% at the beginning of the observation period (from $12 \, mm^{-1}$ to 8–$9 \, mm^{-1}$) and exhibited similar patterns for both storage temperatures (Fig. 2). We estimate SSA measurement error to be ~5%. Snow composed of small rounded grains has been shown to have similar SSA values. Kaempfer and Schneebeli (2007) and Löwe and others (2011) reported SSA values of 9–$12 \, mm^{-1}$ for snow having a volume density of 50%. These earlier studies also found that the SSA of rounded-grain snow decreased over time (Kaempfer and Schneebeli, 2007; Löwe and others, 2011).

We measured specific grain boundary areas (SGBAs) ranging from 1 to $2 \, mm^{-1}$. This parameter showed no detectable change during the experiment. The specific internal grain boundary area (SIGBA) was initially ~$8.5 \, mm^{-1}$ and decreased by almost 40% to ~$5 \, mm^{-1}$ after 27 weeks (Fig. 3). We estimated the error in SGBA measurements to be 5–10%. The total SGBA (SGBA + SIGBA) ranged from 7 to $9 \, mm^{-1}$. We compared GBA measurements from the laboratory ice beads with those of natural snow. Snow composed of small rounded grains had
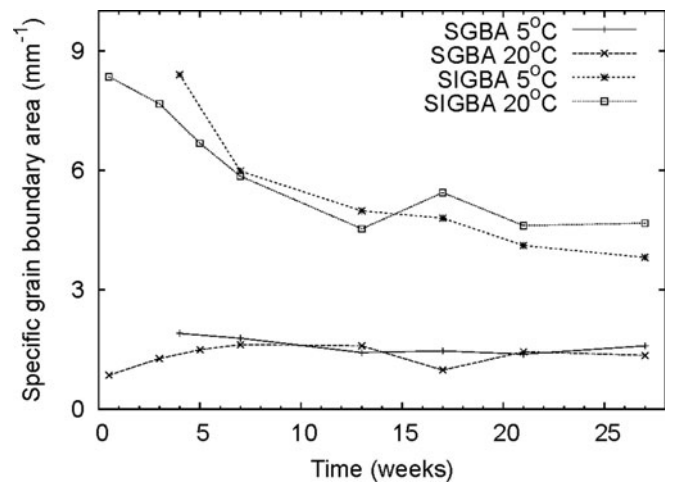
a total specific GBA of 2–$3 \, mm^{-1}$, which is one-third of the corresponding values measured for the ice beads. The ice beads had approximately the same volumetric density as the natural rounded-grain snow.

We found that GBs at neck sites remained mostly unchanged throughout the experiment. The IGBA, however, fell by ~40% during the first 15 weeks, with no measurable change afterwards. The decrease in IGBA for the polycrystalline ice beads is probably due to GB migration. The surface energy of the smaller internal grains is much larger than that of the large grains, and larger grains may encapsulate smaller grains (Berry and others, 1991; Gottstein and others, 1998; Schönfelder and others, 2005).

Hypothetical trace gas diffusion into GBs (Huthwelker and others, 2006) would depend on the extent of GBs and their evolution with time. Analysis of these two factors facilitates the extrapolation of laboratory results to conditions in the natural environment. The polycrystalline structure of the ice beads is likely to produce a greater number of GBs relative to the monocrystalline structure of natural snow (Takahashi and Fujino, 1976). Ice beads apparently have approximately the same GBA as natural snow. Polycrystalline ice, however, is likely to differ from natural snow in terms of its IGBA. The GBA and IGBA exert similar effects on the chemical properties of ice and snow, but IGBA is not geometrically visible. The contrasting IGBA of ice beads and natural rounded-grain snow provides important constraints for experiments concerning snow types with similar SSA but different GBA.

Our experiments also indicate that IGBA evolves primarily during an initial 10–15 week period, with little change observed in the ensuing weeks and months. Different batches of ice beads may vary in their adherence to these findings, and thus require careful monitoring of initial experimental conditions. Large batches of ice beads, however, are expected to show consistent internal structure after 10–15 weeks.

WSL Institute for Snow and F. RICHE
Avalanche Research SLF,
Davos-Dorf, Switzerland
E-mail: riche@slf.ch

Paul Scherrer Institute, T. BARTELS-RAUSCH
Villigen, PSI, Switzerland S. SCHREIBER*
M. AMMANN

*Swiss Federal Institute of Technology,
Zürich, Switzerland

WSL Institute for Snow and M. SCHNEEBELI
Avalanche Research SLF,
Davos-Dorf, Switzerland
E-mail: schneebeli@slf.ch

12 April 2012

REFERENCES

Barret M, Houdier S and Domine F (2011) Thermodynamics of the formaldehyde–water and formaldehyde–ice systems for atmospheric applications. *J. Phys. Chem. A,* **115**(3), 307–317 (doi: 10.1021/jp108907u)

Bartels T, Eichler B, Zimmermann P, Gäggeler HW and Ammann M (2002) The adsorption of nitrogen oxides on crystalline ice. *Atmos. Chem. Phys.,* **2**(3), 235–247 (doi: 10.5194/acp-2-235-2002)

Bartels-Rausch T, Guimbaud C, Gäggeler HW and Ammann M (2004) The partitioning of acetone to different types of ice and snow between 198 and 223 K. *Geophys. Res. Lett.,* **31**(16), L16110 (doi: 10.1029/2004GL020070)

Berry RS, Bernholc J and Salamon P (1991) Disappearance of grain boundaries in sintering. *Appl. Phys. Lett.,* **58**(6), 595–597 (doi: 10.1063/1.105222)

Domine F and Shepson PB (2002) Air–snow interactions and atmospheric chemistry. *Science,* **297**(5586), 1506–1510 (doi: 10.1126/science.1074610)

Domine F and 7 others (2008) Snow physics as relevant to snow photochemistry. *Atmos. Chem. Phys.,* **8**(2), 171–208 (doi: 10.5194/acp-8-171-2008)

Gottstein G, Molodov DA and Shvindlerman LS (1998) Grain boundary migration in metals: recent developments. *Interface Sci.,* **6**(1–2), 7–22 (doi: 10.1023/A:1008641617937)

Grannas AM and 34 others (2007) An overview of snow photochemistry: evidence, mechanisms and impacts. *Atmos. Chem. Phys.,* **7**(16), 4329–4373 (doi: 10.5194/acp-7-4329-2007)

Huthwelker T, Ammann M and Peter T (2006) The uptake of acidic gases on ice. *ChemInform,* **37**(25) (doi: 10.1002/chin.200625216)

Kaempfer TU and Schneebeli M (2007) Observation of isothermal metamorphism of new snow and interpretation as a sintering process. *J. Geophys. Res.,* **112**(D24), D24101 (doi: 10.1029/2007JD009047)

Kerbrat M, Pinzer B, Huthwelker T, Gäggeler HW, Ammann M and Schneebeli M (2008) Measuring the specific surface area of snow with X-ray tomography and gas adsorption: comparison and implications for surface smoothness. *Atmos. Chem. Phys.,* **8**(5), 1261–1275 (doi: 10.5194/acp-8-1261-2008)

Kerbrat M, Huthwelker T, Gäggeler HW and Ammann M (2010) Interaction of nitrous acid with polycrystalline ice: adsorption on the surface and diffusion into the bulk. *J. Phys. Chem. C,* **114**(5), 2208–2219 (doi: 10.1021/jp909535c)

Löwe H, Spiegel JK and Schneebeli M (2011) Interfacial and structural relaxations of snow under isothermal conditions. *J. Glaciol.,* **57**(203), 499–510 (doi: 10.3189/002214311796905569)

Mulvaney R, Wolff EW and Oates K (1988) Sulphuric acid at grain boundaries in Antarctic ice. *Nature,* **331**(6153), 247–249 (doi: 10.1038/331247a0)

Riche F and Schneebeli M (in press) Design-based stereology to quantify structural properties of artificial and natural snow using thin sections. *Cold Reg. Sci. Technol.* (doi: 10.1016/j.coldregions.2012.03.008)

Schönfelder B, Gottstein G and Shvindlerman LS (2005) Comparative study of grain-boundary migration and grain-boundary self-diffusion of twist-grain boundaries in copper by atomistic simulations. *Acta Mater.,* **53**(6), 1597–1609 (doi: 10.1016/j.actamat.2004.12.010)

Takahashi Y and Fujino K (1976) Crystal orientation of fabrics in a snow pack. *Low Temp. Sci., Ser. A* 34, 71–78

Theile T and Schneebeli M (2011) Algorithm to decompose three-dimensional complex structures at the necks: tested on snow structures. *IET Image Process.,* **5**(2), 132–140 (doi: 10.1049/iet-ipr.2009.0410)

Tschanz SA, Burri PH and Weibel ER (2011) A simple tool for stereological assessment of digital images: the STEPanizer. *J. Microsc.,* **243**(1), 47–59 (doi: 10.1111/j.1365-2818.2010.03481.x)